Multiple formation mechanisms of ferrous olivine in CV carbonaceous chondrites during fluid-assisted metamorphism

Alexander N. Krot[1]*, Michail I. Petaev[2] and Phil A. Bland[3]

[1] *Hawai'i Institute of Geophysics and Planetology, School of Ocean and Earth Science and Technology, University of Hawai'i at Manoa, Honolulu, HI 96822, U.S.A.*
[2] *Harvard-Smithsonian Center for Astrophysics and Department of Earth and Planetary Science, Harvard University, Cambridge, MA 02138, U.S.A.*
[3] *Department of Earth Science and Engineering, South Kensington Campus, Imperial College London, SW7 2AZ, U.K.*
Corresponding author. E-mail: sasha@higp.hawaii.edu

Abstract: The CV carbonaceous chondrites experienced alteration that resulted in formation of secondary ferrous olivine (Fa_{40-100}), salite-hedenbergite pyroxenes (Fs_{10-50} Wo_{45-50}), wollastonite, andradite, nepheline, sodalite, phyllosilicates, magnetite, Fe,Ni-sulfides and Ni-rich metal in their Ca,Al-rich inclusions, amoeboid olivine aggregates, chondrules, and matrices. It has previously been suggested that fibrous ferrous olivine in dark inclusions in CV chondrites formed by dehydration of phyllosilicates during thermal metamorphism (T. Kojima and K. Tomeoka, Geochim. Cosmochim. Acta, **60**, 2651, 1996; A.N. Krot *et al*., Meteoritics, **30**, 748, 1995). This mechanism has been subsequently applied to explain the origin of ferrous olivine in the CV chondrules and matrices (A.N. Krot *et al*., Meteoritics, **32**, 31, 1997). It is, however, inconsistent with the lack of significant fractionation of bulk oxygen isotope compositions of the CV chondrites and the Allende dark inclusions and the common occurrences of ferrous olivine in the aqueously-altered and virtually unmetamorphosed oxidized CV chondrites of the Bali-like subgroup. Based on the petrographic observations and the isotopic compositions of ferrous olivine and coexisting Ca,Fe-rich silicates in CV chondrites and their dark inclusions, we infer that ferrous olivine formed during a fluid-assisted metamorphism by several mechanisms: (*i*) replacement of Fe,Ni-metal±sulfide nodules, (*ii*) replacement of magnesian olivine and low-Ca pyroxene, and (*iii*) direct precipitation from an aqueous solution. Dehydration of phyllosilicates appear to have played only a minor (if any) role. Although our model does not address specifically the origin of ferrous olivine rims around forsterite grains in Allende, the observed homogenization of matrix olivines (which have comparable sizes to thicknesses of the ferrous olivine rims in Allende) from Kaba to Allende suggests that compositions of ferrous olivine rims in Allende cannot be primary and must have been modified by asteroidal alteration.

key words: ferrous olivine, fayalite, asteroidal alteration, Mn-Cr ages, oxygen isotopic compositions

1. Introduction

The CV (Vigarano-type) carbonaceous chondrites are subdivided into the reduced

(CV_{red}) and two oxidized subgroups, Allende-like (CV_{oxA}) and Bali-like (CV_{oxB}) (McSween, 1977; Weisberg *et al.*, 1997), which largely reflect their complex alteration history and may represent different lithologic varieties of the same asteroidal body (Krot *et al.*, 1998a, 2000a).

The CV_{oxB} chondrites (*e.g.*, Kaba, Bali) experienced aqueous alteration that resulted in formation of secondary phyllosilicates, magnetite, Fe,Ni-sulfides, Fe,Ni-carbides, fayalite, salite-hedenbergite pyroxenes ($Fs_{10-50}Wo_{45-50}$), and andradite (Krot *et al.*, 1998a; Hashimoto and Grossman, 1987). The CV_{oxB} matrices (Fig. 1a) largely consist of secondary minerals, including concentrically-zoned nodules of Ca,Fe-pyroxenes and andradite, coarse ($>10\,\mu$m) grains of nearly pure fayalite ($Fa_{>90}$), abundant phyllosilicates, and very fine-grained ($<1-2\,\mu$m) ferrous olivine ($\sim Fa_{50}$).

The CV_{oxA} chondrites (*e.g.*, Allende, ALH84128) are more extensively altered than the CV_{oxB}, but contain very minor phyllosilicates. The major secondary minerals include ferrous olivine (Fa_{40-60}), Ca,Fe-pyroxenes, andradite, wollastonite, kirsch-
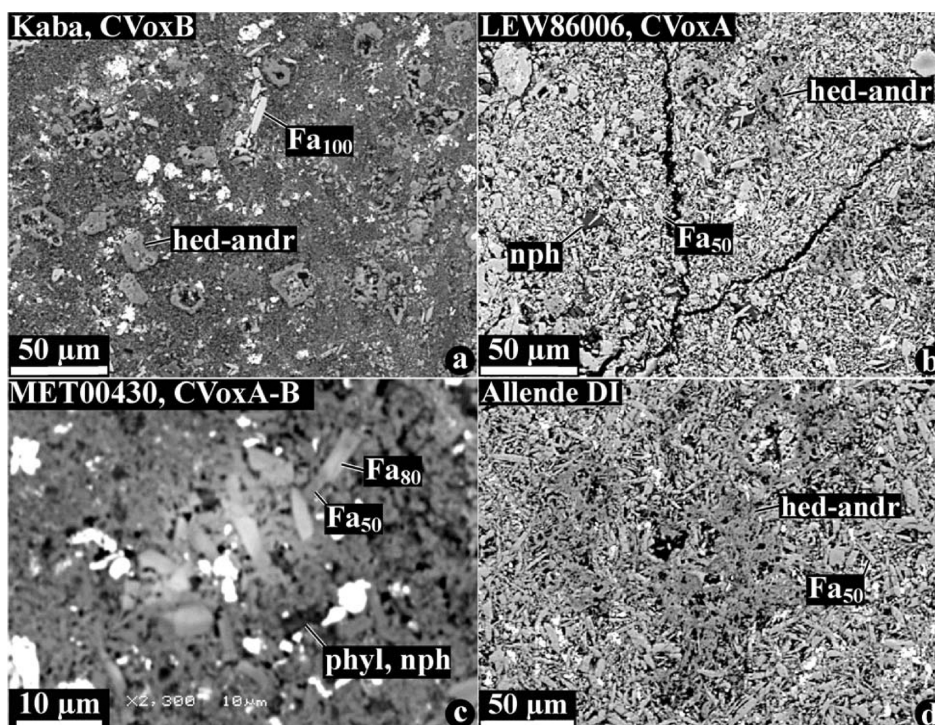

Fig. 1. Backscattered electron (BSE) images of matrices in the oxidized CV chondrites (a–c) and Allende dark inclusion (d). Matrix in the CV_{oxB} Kaba contains nearly pure fayalite ($\sim Fa_{100}$) and very fine-grained groundmass largely composed of ferrous olivine ($\sim Fa_{50}$) and phyllosilicates. Matrix in the CV_{oxA-B} MET00430 contains fayalite grains showing inverse compositional zoning (Fa_{80-50}), finer grained, lath-shaped ferrous olivine ($\sim Fa_{50}$), nepheline and/or phyllosilicates. Matrices in the CV_{oxA} LEW86006 and Allende dark inclusion IV-1 contain relatively coarse-grained, lath-shaped compositionally uniform ($\sim Fa_{50}$) ferrous olivine and nepheline. All matrices contain Ca,Fe-pyroxenes-andradite (hed-andr) nodules.

steinite, nepheline, sodalite, Fe,Ni-sulfides, magnetite, and Ni-rich metal (Krot *et al.*, 1998a; Hashimoto and Grossman, 1987). The CV_{oxA} matrices (Fig. 1b) are coarser-grained than those in the CV_{oxB} chondrites and largely consist of Ca,Fe-pyroxene $\pm$ andradite nodules, lath-shaped ferrous olivine (~Fa_{50}), and nepheline.

Some oxidized CVs (*e.g.*, MET00430) are mineralogically intermediate between the CV_{oxB} and CV_{oxA} chondrites (Krot *et al.*, 2003a, b). For example, chondrules in MET 00430 contain both phyllosilicates and nepheline (Krot, unpubl.), whereas its matrix (Fig. 1c) contains ferrous olivine with grain sizes intermediate between those in the matrices of the CV_{oxA} and CV_{oxB} chondrites and with inverse compositional zoning (Fa_{80-50}).

The Mokoia meteorite is a complex breccia containing clasts of CV_{oxA} and CV_{oxB} materials and heavily-metamorphosed oxidized chondritic clasts (Krot *et al.*, 1998a). The CV_{oxA} clasts experienced aqueous alteration that overprints "anhydrous" Allende-like alteration: phyllosilicates replace nepheline and sodalite (Kimura and Ikeda, 1998).

The reduced CV chondrites Efremovka and Leoville experienced alteration similar to that of the CV_{oxA} meteorites, but of a smaller degree. Both meteorites virtually lack phyllosilicates and contain nepheline, sodalite, and salite-hedenbergite pyroxenes; however, these minerals are much less abundant than in the Allende-like meteorites. The reduced CV chondrite breccia Vigarano contains clasts of the CV_{oxB} and CV_{oxA} materials (Krot and Todd, 1998; Krot *et al.*, 2000a); the reduced portion experienced aqueous alteration resulting in formation of phyllosilicates and magnetite.

In addition to the oxidized and reduced subgroups, the CV chondrites contain lithic chondrite clasts (often called "dark inclusions") which are chemically and petrographically similar to their host meteorites (Fig. 1d), but generally experienced more extensive alteration (*e.g.*, Fruland *et al.*, 1978; Kracher *et al.*, 1985; Kurat *et al.*, 1989; Johnson *et al.*, 1990; Krot *et al.*, 1995, 1997, 1998a, 1999, 2001; Buchanan *et al.*, 1997; Brearley, 1998). For example, many dark inclusions in Allende consist almost entirely of the secondary ferrous olivine, nepheline, sodalite, Ca,Fe-rich silicates, and Fe,Ni-sulfides (Krot *et al.*, 2001).

The origin of secondary mineralization in CV chondrites remains controversial; nebular and asteroidal models have previously been proposed (*e.g.*, Palme and Wark, 1988; Kimura and Ikeda, 1995; Krot *et al.*, 1995, 1997, 1998a, b; Weisberg and Prinz, 1998; Dohmen *et al.*, 1998; Brearley, 2003). According to the nebular model (Palme and Wark, 1988; Kimura and Ikeda, 1995; Weisberg and Prinz, 1998; Dohmen *et al.*, 1998), the CV_{oxA} chondrules and refractory inclusions were exposed to a highly oxidized nebular gas resulting in their alteration; matrix minerals, including ferrous olivine, directly condensed from this gas. We note that arguments favoring the nebular model is largely based on the presence of ferrous olivine rims around forsteritic olivines in Allende with a steep compositional gradient between the rims and the host olivine grains. The similar rims have been experimentally reproduced at high temperatures by Dohmen *et al.* (1998). In addition, Brenker *et al.* (2000) provided strong mineralogical evidence for high-temperature origin of at least some of the Ca,Fe-rich pyroxene–andradite nodules in the Allende matrix, which appears to be consistent with the nebular model*

---

*Brenker and Krot (2004) recently reported textural and mineralogical evidence for an asteroidal, high-temperature and low-temperature origin of Ca,Fe-rich pyroxene-andradite-wollastonite assemblages in Allende.

as well. This model is, however, inconsistent with (*i*) the extensive petrographic evidence for asteroidal alteration of the CV chondrites and Allende dark inclusions, including veins, chondrule pseudomorphs and Ca,Fe-rich rims around dark inclusions composed of the secondary minerals observed in the Allende host (*e.g.*, Kojima and Tomeoka, 1996; Krot *et al.*, 1997a, 1998a, b, 1999, 2001, 2002), (*ii*) the presence of poorly-graphitized carbon (PGC) and pentlandite inclusions in matrix olivine, which are unstable at high temperatures (Brearley, 1999), (*iii*) the lack of volatility-controlled rare earth element (REE) patterns in matrix Ca,Fe-pyroxenes and andradite (Brearley and Shearer, 2000), and (*iv*) the large mass-dependent fractionation of oxygen isotopes ($\delta^{18}O \sim 20‰$) in secondary fayalite, magnetite, Ca,Fe-rich pyroxenes, and andradite, suggesting that alteration occurred at low temperatures (Krot *et al.*, 2000b; Choi *et al.*, 2000; Cosarinsky *et al.*, 2003), and (*v*) the prolong duration (~14 Ma) of the CV alteration (Pravdivtseva and Hohenberg, 2001; Pravdivtseva *et al.*, 2001, 2003a, b; Krot *et al.*, 2003c), which is inconsistent with the inferred life-time of the solar nebula (Podosek and Cassen, 1994).

According to the asteroidal models (Kojima and Tomeoka, 1996; Krot *et al.*, 1995, 1997, 1998a, b, 2003a, b), CV chondrites experienced fluid-assisted thermal metamorphism of various degrees, which resulted in mobilization of Ca, Si, Fe, Mg, Mn, Na, and S, and replacement of primary phases in chondrules, CAIs and matrices by secondary minerals. It was originally suggested that secondary ferrous olivine in dark inclusions in CV chondrites formed by dehydration of phyllosilicates during thermal metamorphism (Kojima and Tomeoka, 1996; Krot *et al.*, 1995). This mechanism has been subsequently applied to explain the origin of ferrous olivine in the CV chondrules and matrices (Krot *et al.*, 1997). However, this mechanism appears to be inconsistent with the lack of mass-dependent fractionation of oxygen isotopes in bulk CV chondrites (Clayton and Mayeda, 1999), which is expected for the extensively aqueously-altered and dehydrated meteorites (*e.g.*, metamorphosed CI/CM chondrites). In addition, this model does not explain steep compositional gradients between the ferrous olivine rims and their host chondrules in Allende. Later, Krot *et al.* (1998a, b, 2000b, 2001, 2002) concluded that Ca, Fe, Mg, and Si were dissolved and mobilized by a fluid phase (aqueous solution) from which these elements subsequently precipitated as the secondary Ca,Fe-rich minerals (salite-hedenbergite pyroxenes, wollastonite, andradite, and kirschsteinite) in chondrules, CAIs, and matrices of the CV chondrites. Here, we conclude that secondary ferrous olivine in CV chondrites formed by the same process—fluid-assisted metamorphism—*via* several mechanisms: (*i*) replacement of opaque nodules, (*ii*) replacement of magnesian olivine and pyroxene, and (*iii*) direct precipitation from a fluid. Dehydration of phyllosilicates appears to have played only a minor (if any) role.

2.   Analytical procedures

Polished thin sections of the oxidized CV chondrites Allende, Kaba, Mokoia, ALH 84028, LEW86006, and MET00430 were studied by optical microscopy and in the backscattered electron (BSE) mode with a JEOL JSM 5900LV scanning electron microscope. Mineral compositions were measured with a fully focused (1–2 μm) beam

with a Cameca SX50 electron microprobe using 15 kV accelerating voltage and 10–20 nA beam current. Counting times on both peak and background were 10 s for Na and K and 20 s for all other elements. Well-characterized silicates and oxides were used as standards. Matrix corrections were applied using a PAP software routine. Detection limits in silicates were (in wt%): SiO_2, Al_2O_3, MgO—0.03; TiO_2, CaO, K_2O—0.04; Na_2O, Cr_2O_3—0.06; MnO—0.07; FeO—0.08.

3.   Results and discussion

In the following sections, we summarize the mineralogical, petrographic and isotopic evidence for multiple formation mechanisms (listed above) of the secondary ferrous olivine in the oxidized CV chondrites and CV dark inclusions during fluid-assisted metamorphism. The origin of fibrous ferrous olivine in an Allende dark inclusion by dehydration of phyllosilicates has previously been discussed in by Kojima and Tomeoka (1996) and we only briefly summarize arguments in favor and against this mechanism. Because CAIs, AOAs, and chondrules in the reduced CV chondrites Efremovka and Leoville experienced relatively small degrees of the Allende-like alteration and because their matrices were extensively modified by shock metamorphism (Scott *et al.*, 1992), they are not discussed in this paper.

3.1.   Replacement of opaque nodules in Type I chondrules

Type I chondrules in primitive ordinary (*e.g.*, LL3.0 Semarkona) and carbonaceous (*e.g.*, CR and CO3.0 chondrites) consist of magnesian olivine and low-Ca pyroxene phenocrysts, abundant Fe,Ni-metal nodules, and glassy mesostasis with or without high-Ca pyroxene crystallites (*e.g.*, Jones and Scott, 1989; Brearley and Jones, 1998; Krot *et al.*, 2002). In contrast, the opaque nodules in Type I chondrules in the CV_{oxB} chondrites Kaba and Mokoia consist of magnetite, Fe,Ni-sulfides, fayalite ($Fa_{>90}$) and Ca,Fe-pyroxenes; tiny relict grains of Ni-rich metal surrounded by ferrous olivine haloes are found inside forsterite phenocrysts (Fig. 2a, b). The fayalite and Ca,Fe-pyroxenes replace magnetite-sulfide nodules and contain relict grains of magnetite and sulfides (Figs. 2a, b, 6a, b). The presence of sulfides inside fayalite excludes its high-temperature formation. Fayalite has high MnO contents (up to 1.5 wt%); Cr_2O_3 contents are generally below the detection limit of electron probe microanalysis (<0.06 wt%). Fine-grained rims around some of the chondrules are crosscut by fayalite-magnetite veins, which start at the opaque nodules in chondrule peripheries (Fig. 2c, d). These observations indicate that fayalite formation postdates accretion of the fine-grained chondrule rims and that Fe in the veins was supplied by alteration of the opaque nodules. We note that similar textural occurrences of secondary fayalite and Ca,Fe-pyroxenes have been described from the ungrouped carbonaceous chondrite MAC88107, where these phases unambiguously formed by *in situ* aqueous alteration (Krot *et al.*, 2000a).

The unaltered Type I chondrules in primitive ordinary and carbonaceous chondrites contain abundant Fe,Ni-metal nodules; magnetite is absent. Moreover, the oxygen isotopic compositions of magnetite in the Kaba and Mokoia chondrules are in disequilibrium with the chondrule phenocrysts (Choi *et al.*, 2000), implying that magnetite is a secondary mineral formed by oxidation of Fe,Ni-metal:
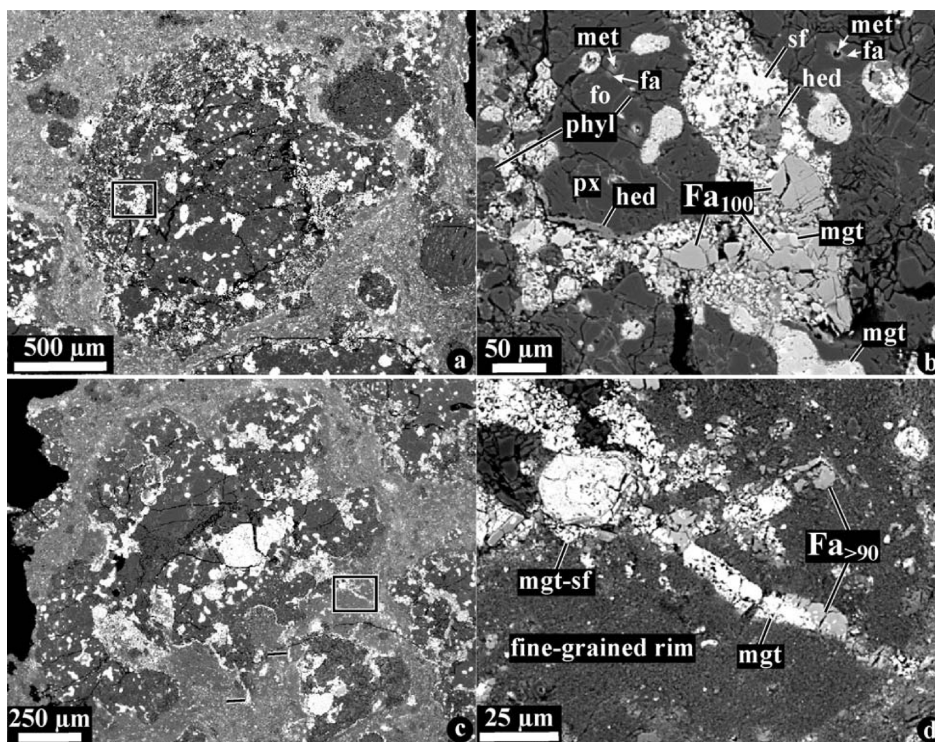
Fig. 2. *BSE images of secondary ferrous olivine in and around Type I porphyritic olivine-pyroxene chondrules in the CV$_{oxB}$ chondrite Mokoia.   a, b—Opaque nodules (originally Fe,Ni-metal$\pm$ troilite) are replaced by magnetite (mg), Ni-bearing sulfides (sf), fayalite (Fa$_{>90}$), and salite-hedenbergite pyroxenes (hed); chondrule mesostasis is replaced by phyllosilicates (phyl). Fayalite and salite-hedenbergite pyroxenes replace magnetite.   Relict Ni-rich metal inclusions in forsterite (fo) are surrounded by halloes of ferrous (Fa$_{~50}$) olivine (fa).   c, d—Chondrule surrounded by a continuous fine-grained rim crosscut by the fayalite (Fa$_{>90}$)–magnetite (mgt) veins that start at the opaque nodules in the peripheral portion of the chondrule composed of Ni-bearing sulfide and magnetite.   Regions outlined in "a" and "c" are shown in detail in "b" and "d", respectively.*

$$3Fe_{(s)} + 4H_2O_{(l,g)} = Fe_3O_{4(s)} + 4H_{2(g)}, \qquad (1)$$

where s=solid, l=liquid, g=gas.

On a three-oxygen isotope plot (Fig. 3), O-isotopic compositions of fayalite and magnetite in the Kaba and Mokoia chondrules plot along the terrestrial fractionation line and have similar values of $\Delta^{17}O$, suggesting formation from the same oxygen isotope reservoir.   The $\delta^{18}O$ values of fayalite grains are ~10–20‰ heavier than those of the coexisting magnetite nodules, indicating formation at low ($<300°C$) temperatures (Hutcheon *et al*., 1998; Krot *et al*., 1998a; Choi *et al*., 2000).   We note that the secondary Ca,Fe-rich silicates in Allende and the Allende dark inclusions have a similar range of $\delta^{18}O$ and $\Delta^{17}O$ values (Krot *et al*., 2000b; Cosarinsky *et al*., 2003), suggesting a similar environment of alteration.
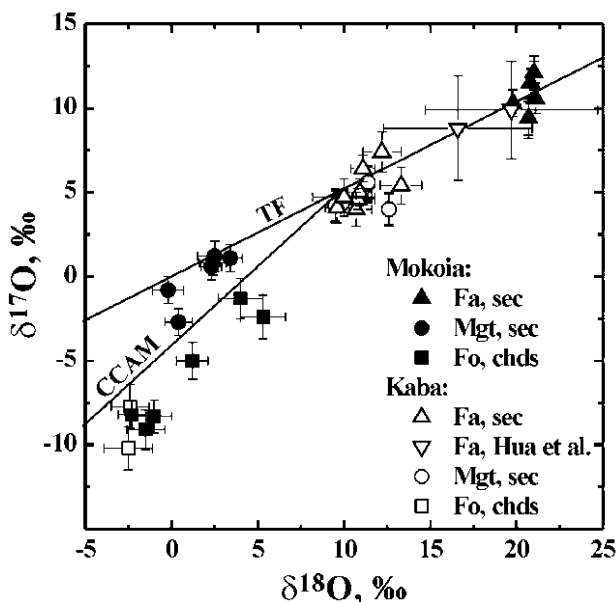
Fig. 3. Oxygen isotopic compositions of secondary magnetite (Mgt) and fayalite (Fa), and primary forsteritic olivine (Fo) in Type I chondrules in the CV_{oxB} chondrites Kaba and Mokoia (data from Choi et al., 2000; Hua et al., 2003). The terrestrial fractionation (TF) line and carbonaceous chondrite anhydrous mineral (CCAM) line are shown for reference. In Mokoia, the magnetite and fayalite differ in $\delta^{18}O$ by ~20‰, suggesting formation at low-temperature. In Kaba, the compositions of fayalite and magnetite reported by Choi et al. (2000) are nearly identical, and very close to the intersection of the TF and CCAM lines. The compositions of Kaba fayalites reported by Choi et al. (2000) are inconsistent with those reported by Hua et al. (2003); the latter are similar to those of Mokoia fayalites. We note that compositions of fayalite and magnetite in Kaba reported by Choi et al. (2000) were collected with a 3 months interval and might be in error. Compositions of forsteritic olivine phenocrysts plot along CCAM line and are in disequilibrium with those of the secondary minerals.

Because Si is not a volatile element, formation of fayalite by replacement of Si-free magnetite suggests that Si must have been transported through an aqueous (aq) solution (small amount of Si might have been dissolved in Fe,Ni-metal subsequently replaced by magnetite):

$$2Fe_3O_{4(s)} + 3SiO_{2(aq)} + 2H_{2(g)} = 3Fe_2SiO_{4(s)} + 2H_2O_{(l,g)}, \qquad (2)$$

rather than through a high-temperature vapor phase implied by the nebular model:

$$2Fe_3O_{4(s)} + 3SiO_{(g)} + H_2O_{(g)} = 3Fe_2SiO_{4(s)} + H_{2(g)}. \qquad (3)$$

The proposed mechanism of the fayalite formation is consistent with the presence of abundant phyllosilicates in the CV_{oxB} chondrules and could explain the observed fractionation of both refractory Ca and Al in Ca,Fe-rich silicates and moderately volatile Mn and Cr in fayalite. These fractionations are commonly observed in CI and
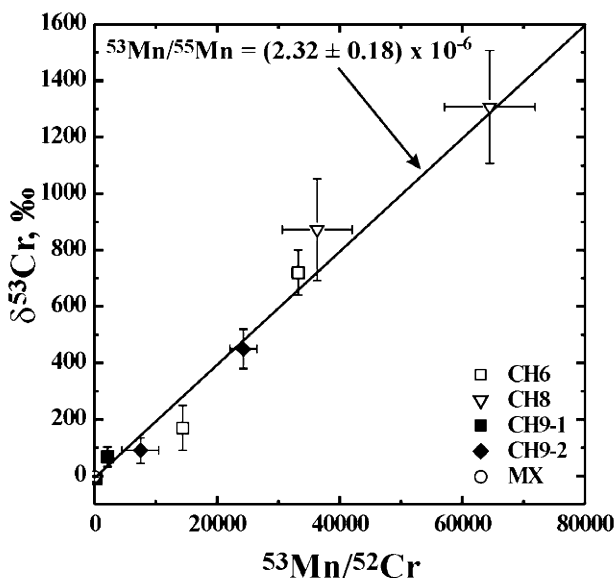
Fig. 4. ^{53}Mn-^{53}Cr evolution diagram for four fayalite grains in three porphyritic olivine-pyroxene Type I chondrules and a matrix material from the CV_{oxB} chondrite Mokoia. Slope of the line fitted to all data yields the initial $^{53}Mn/^{55}Mn$ ratio at the time of fayalite formation of $(2.32\pm0.18)\times10^{-6}$. Errors are two standard deviations (from Hutcheon et al., 1998).

CM carbonates (Brearley and Hutcheon, 2000, 2002) and may have resulted from differences in the solubility of these elements in aqueous solutions.

Fayalite in Mokoia chondrules shows excesses of ^{53}Cr (decay product of ^{53}Mn; $t_{1/2}$ ~3.7 Ma) corresponding to the initial $^{53}Mn/^{55}Mn$ ratio of $(2.32\pm0.18)\times10^{-6}$ (Fig. 4; Hutcheon et al., 1998). This ratio means that the Mokoya fayalite is 3.0 ± 0.7 Ma older than the angrite LEW86010 having an absolute Pb-Pb age of 4557.8 ± 0.5 Ma (Lugmair and Shukolyukov, 1998). Because the absolute Pb-Pb age of the CV CAIs is $4567.2\pm$ 0.6 Ma (Amelin et al., 2002), the relatively young Mn-Cr ages of the Mokoia fayalites (~7 Ma after CAIs) are consistent with an asteroidal, rather than a nebular, origin. We note, however, that because the life-time of the solar nebula is poorly-constrained (e.g., Podosek and Cassen, 1994; Boss, 2003), these ages alone cannot be considered as a definitive indicator of the environment of alteration; mineralogical, petrographic and O-isotope studies are more important.

The opaque nodules in Type I chondrules in the CV_{oxA} chondrites (Fig. 5a, b) and Allende dark inclusions (Fig. 5c) are more extensively replaced by Ca,Fe-pyroxenes and ferrous olivine than those in the CV_{oxB} chondrules: relict sulfides are common, whereas magnetite is virtually absent. This is consistent with the low abundance of magnetite in the CV_{oxA} chondrites compared to the CV_{oxB} (Bland et al., 2000). Fine-grained rims around chondrules are commonly crosscut by veins composed of ferrous olivine, Ca,Fe-pyroxenes, and sulfides (Fig. 5c; Krot et al., 1998a, b). Both textural varieties of ferrous olivine in the CV_{oxA} chondrites are more magnesian (Fa$_{40-60}$) than those replacing opaque nodules in the CV_{oxB} chondrules (Fa$_{>90}$). Ferrous olivine replacing
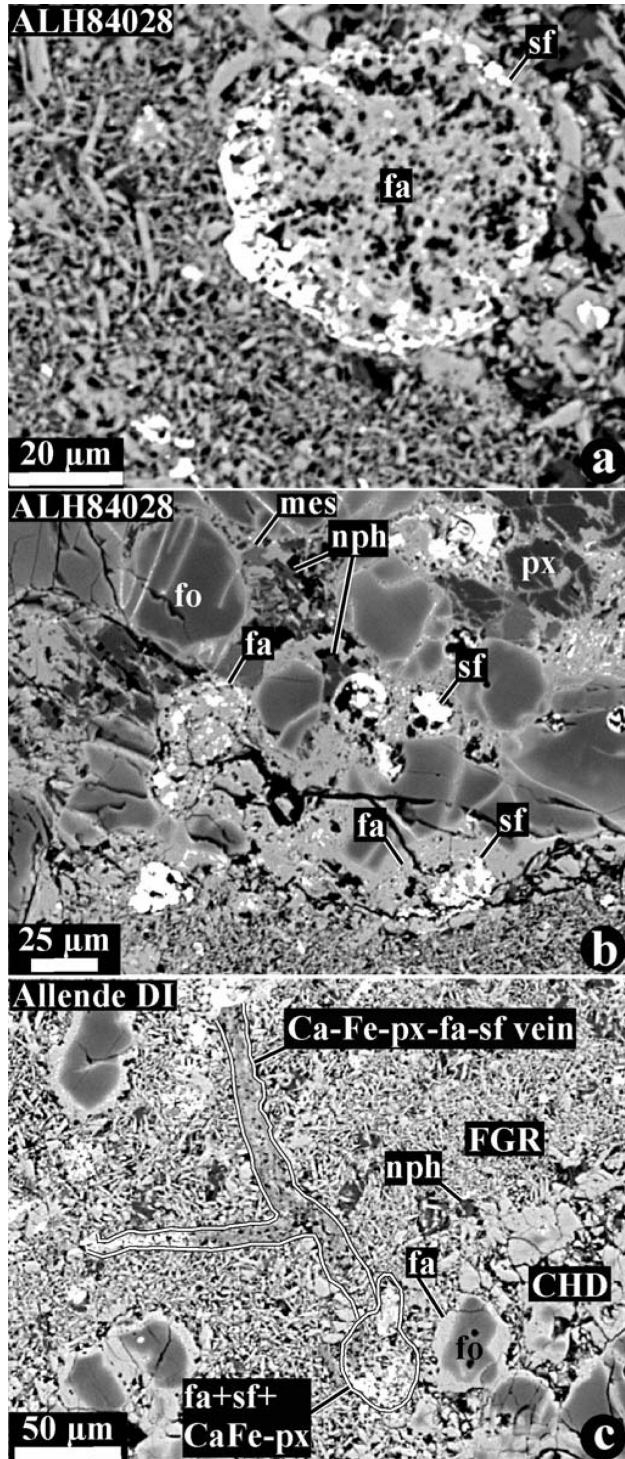
Fig. 5. BSE images of altered chondrules in the CV_{oxA} chondrite ALH 84028 (a, b) and in the Allende dark inclusion (DI) 3529. Opaque nodules in the chondrules are replaced by ferrous (Fa_{-50}) olivine (fa) and Fe,Ni-sulfides (sf). Low-Ca pyroxene (px) phenocrysts are replaced by ferrous olivine; chondrule mesostasis (mes) is replaced by nepheline (nph). Chondrule (CHD) in the Allende dark inclusion is surrounded by a fine-grained rim (FGR) composed of lath-shaped ferrous olivine and nepheline. The rim is crosscut by a vein composed of Ca,Fe-pyroxenes (Ca,Fe-px), ferrous olivine and Fe,Ni-sulfides. The vein starts at the opaque nodule (outlined) that is replaced by the Ca,Fe-pyroxenes, ferrous olivine, and Fe,Ni-sulfides.

opaque nodules in the CV_{oxA-B} chondrite MET00430 are characterized by intermediate values of fayalite contents ($Fa_{\sim60-80}$). The observed decrease in fayalite content of secondary olivine from CV_{oxB} ($Fa_{>90}$) to CV_{oxA-B} ($Fa_{\sim60-80}$) to CV_{oxA} ($Fa_{\sim40-60}$) could be either due to an increase in the alteration temperature or due to subsequent re-equilibration between ferrous and magnesian olivines, either through a fluid during aqueous alteration or by a solid state diffusion during thermal metamorphism.

3.2. Replacement of magnesian pyroxene and olivine in chondrules

Forsteritic phenocrysts in Type I chondrules in the CV_{oxB} chondrites show a small degree of replacement by ferrous olivine at the contact with fayalite grains (Fig. 6a, b). There is a sharp compositional boundary between the ferrous olivine (Fa_{63}) and the replaced forsterite (Fa_1). The neighboring fayalite replacing magnetite-sulfide nodule shows enrichment in a forsterite component (up to Fa_{87}) along the boundary and along the crosscutting veins, suggesting that Mg released during alteration of forsterite diffused into fayalite (Fig. 6b). The original outlines of the forsterite phenocrysts are well-preserved (indicated by arrows in Fig. 6b), suggesting that they are pseudomorphed by ferrous olivine. The pseudomorphic replacement of forsterite requires extensive mobilization of Fe, Mg, and Si, which may have occurred either through a high-temperature gas or a low-temperature aqueous solution. The high-temperature reactions are inconsistent with the observations indicating that alteration postdates accretion of fine-grained rims around chondrules showing no evidence for high-temperature processing (Krot *et al.*, 1998a; Choi *et al.*, 2000). The presence of abundant phyllosilicates coexisting with fayalite in the fayalite-bearing chondrules in the CV_{oxB} chondrites suggests that Fe-Mg interdiffusion in forsterite and fayalite took place in the presence of aqueous solutions, possibly by the following reactions:

$$Fe^{2+}_{(aq)} + Mg_2SiO_{4(s)} + H_2O_{(l,g)} = (Fe,Mg)_2SiO_{4(s)} + Mg^{2+}_{(aq)} + H_{2(g)}, \qquad (4)$$

$$Mg^{2+}_{(aq)} + Fe_2SiO_{4(s)} + H_2O_{(l,g)} = (Fe,Mg)_2SiO_{4(s)} + Fe^{2+}_{(aq)} + H_{2(g)}. \qquad (5)$$

We note, however, that there are no experimental data for diffusion of Fe in olivine in a wet environment.

The supporting arguments in favor of this mechanism come from the aqueously altered Efremovka dark inclusions, where ferrous olivine ($Fa_{\sim50}$) replacing chondrule phenocrysts (Fig. 6c) coexists with very minor phyllosilicates (Krot *et al.*, 1999). Some of the chondrules are completely pseudomorphed by a mixture of ferrous olivine and phyllosilicates (Fig. 6d).

Chondrule phenocrysts in the CV_{oxA} chondrites and Allende dark inclusions are more extensively replaced by ferrous olivine ($Fa_{\sim50}$) than those in the CV_{oxB} chondrites; ferrous olivine contains abundant inclusions of Fe,Ni-sulfides (Figs. 5b, c, 6d–f). Low-Ca pyroxene phenocrysts are more altered than forsteritic olivine phenocrysts. A TEM study of the porphyritic olivine-pyroxene chondrules in Allende (Brearley, 1997) revealed the common presence of talc and amphibole in the low-Ca pyroxene phenocrysts. The presence of hydrous minerals and Fe,Ni-sulfides associated with ferrous olivine in the Allende chondrules suggests that Fe was transported by a low-temperature aqueous solution, possibly by reactions 4 and 6:
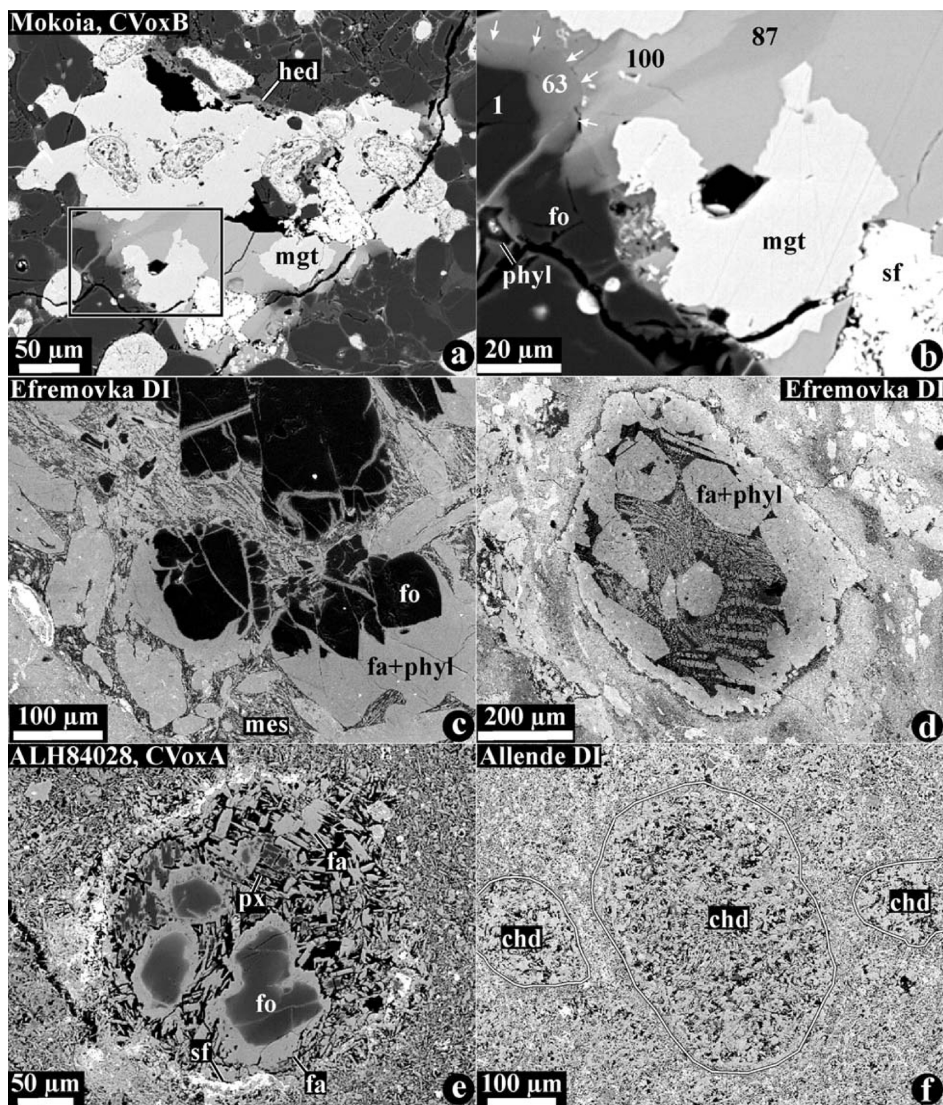
Fig. 6. BSE images of the altered chondrules in the CV_{oxB} chondrite Mokoia (a, b), Efremovka dark inclusion E53 (c, d), CV_{oxA} chondrite ALH84028 (e), and Allende dark inclusion 4301-2 (f). a, b—Numbers correspond to fayalite content (in mol%). Magnetite (mg)—sulfide (sf) nodule is replaced by a nearly pure fayalite ($Fa_{~100}$); forsterite phenocrysts (Fa_1) are partly pseudomorphed by ferrous olivine (Fa_{63}); an outline of one of the grains is indicated by arrows. Fayalite is crosscut by a vein of ferrous olivine (Fa_{87}), suggesting that Mg comes from the replaced forsterite. c, d—Chondrule phenocrysts and mesostases (mes) are pseudomorphed to a various degree by a fine-grained mixture of ferrous olivine (fa) and very minor phyllosilicates (phyl). e—Low-Ca pyroxene phenocrysts are replaced by ferrous ($Fa_{~50}$) olivine (fa); forsteritic olivine (fo) phenocrysts are surrounded by ferrous olivine rims and show moderate enrichment in FeO, largely along fractures. Abundant inclusions of Fe, Ni-sulfides occur in ferrous olivine along chondrule periphery. f—Chondrule pseudomorphs largely composed of ferrous olivine.

$$Fe^{2+}_{(aq)} + MgSiO_{3(s)} + H_2O_{(l,g)} = (Fe,Mg)_2SiO_{4(s)} + H_{2(g)}, \tag{6}$$

rather than by a high-temperature gas (*e.g.*, Dohmen *et al.*, 1998):

$$Fe_{(g)} + MgSiO_{3(s)} + H_2O_{(g)} = (Fe,Mg)_2SiO_{4(s)} + H_{2(g)}. \tag{7}$$

3.3. Direct precipitation from a fluid

Direct precipitation of ferrous olivine from a fluid is indicated by the presence of euhedral ferrous olivines in aqueously-altered AOAs (Fig. 7a, b), CAIs (Fig. 7c, d) and matrices (Fig. 1a) of CV_{oxB} chondrites and by ferrous olivine overgrowths of $CV_{oxB, oxA-B}$
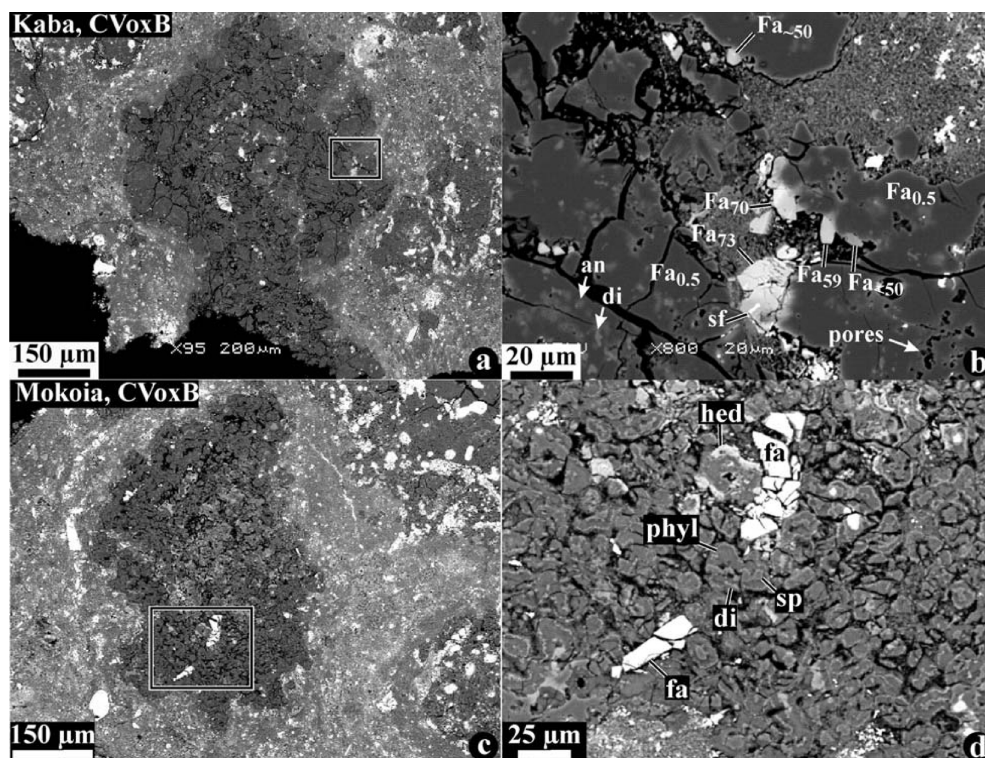

Fig. 7. BSE images of the secondary fayalite formed by a direct precipitation from a fluid in the CV_{oxB} chondrites Kaba and Mokoia. a, b—Amoeboid olivine aggregate composed of forsterite (fo), Al-diopside (di), and anorthite (an). Forsterite grains are overgrown by euhedral ferrous olivines ranging in compositions from $Fa_{<50}$ to Fa_{73}; some of the fayalite grains contain inclusions of Fe,Ni-sulfides (sf). Abundant pores in the outer portion of the AOA are probably due to leaching out of anorthite and Al-diopside. c, d—Fine-grained CAI consisting of concentrically-zoned objects composed of spinel (sp) surrounded by the layers of phyllosilicates (phyl) and Al-diopside (di). The phyllosilicates probably replace anorthite or melilite. Euhedral fayalite ($Fa_{>90}$) grains occur between these bodies; Ca,Fe-pyroxenes (hed) overgrow Al-diopside. Regions outlined in "a" and "c" are shown in detail in "b" and "d", respectively.
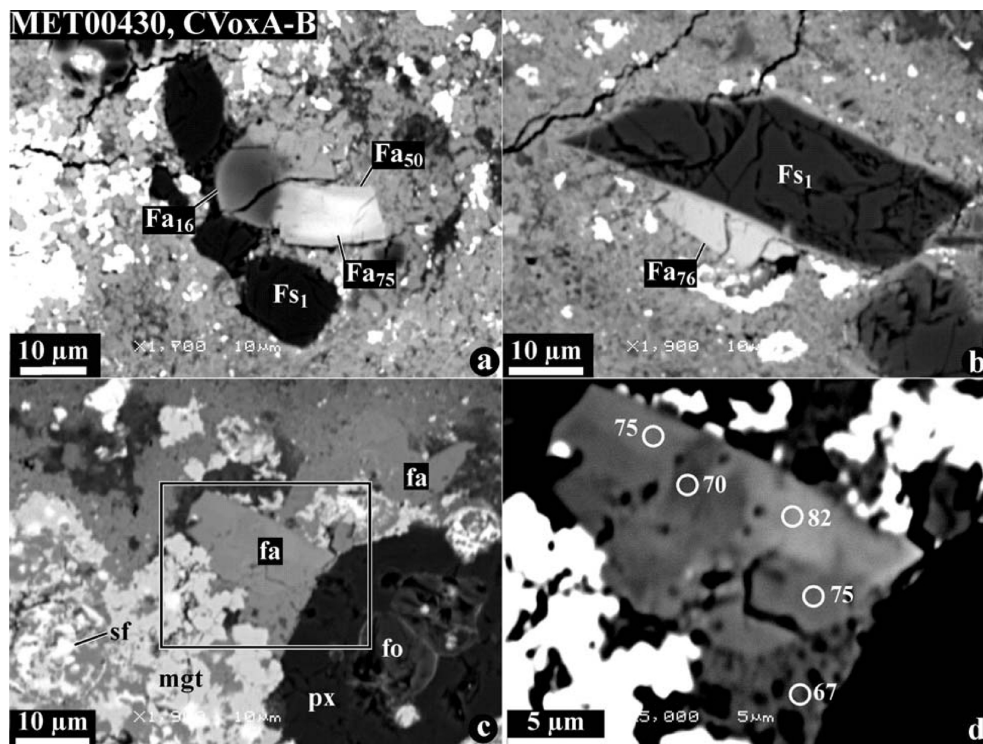
Fig. 8.   *BSE images of the secondary ferrous olivine in the* CV_{oxA-B} *chondrite MET00430.   a—Ferrous olivine overgrowing olivine-pyroxene chondrule fragment shows inverse compositional zoning (Fa_{75-50}).   b—Ferrous olivine overgrowing low-Ca pyroxene grain.   c, d—Euhedral grain of ferrous olivine overgrowing low-Ca pyroxene (px) phenocryst in the outer portion of a Type I porphyritic olivine-pyroxene chondrule shows complex chemical zoning suggesting dissolution of ferrous olivine and precipitation of more forsteritic olivine from a fluid phase. Numbers correspond to fayalite contents (from Krot et al., 2003b).*

chondrules and chondrule fragments (Fig. 8).   Figures 7a and 7b show an aqueously-altered AOA in Kaba that contains primary forsterite, anorthite and Al-diopside. Some of the anorthite and Al-diopside grains are either replaced by phyllosilicates or completely leached out, leaving behind abundant pores.   Forsterite grains in the outer portion of the AOA are overgrown by euhedral grains of ferrous olivine showing significant intergrain variations in chemical compositions ($Fa_{\sim 50-73}$).   Some of the ferrous olivines contain inclusions of Fe,Ni-sulfides, suggesting low-temperature formation of this mineral assemblage.   We infer that these ferrous olivine grains precipitated directly from an aqueous solution:

$$Fe^{2+}{}_{(aq)} + Mg^{2+}{}_{(aq)} + SiO_{2(aq)} = (Fe,Mg)_2SiO_{4(s)}. \tag{8}$$

This mechanism is consistent with the lack of a significant enrichment in fayalite content in the host forsterites.   The observed variations in chemical compositions of the neighboring ferrous olivines suggest that the composition of the fluid (concentration of

Mg^{2+} and Fe^{2+}) was heterogeneous on a local scale ($< 1\,mm$), possibly due to its small abundance.

Figures 7c and 7d show an aqueously-altered, fine-grained, spinel-rich CAI in Mokoia that consists of multiple concentrically-zoned bodies, each composed of spinel surrounded by layers of phyllosilicates and Al-diopside. The phyllosilicates probably replace primary melilite or anorthite, commonly observed in unaltered fine-grained CAIs in primitive carbonaceous chondrites (*e.g.*, Aléon *et al.*, 2002; Krot *et al.*, 2004). Several euhedral grains of fayalite ($Fa_{>90}$) occur between the spinel-phyllosilicate-diopside bodies in the CAI core. The fayalite grains show no evidence for resorbtion by the phyllosilicates, which is consistent with their precipitation from an aqueous solution responsible for the origin of phyllosilicates. Euhedral grains of fayalite are also commonly observed in the CV_{oxB} matrices (Fig. 1a; Hua and Buseck, 1995). These grains are texturally and compositionally similar to fayalite in CAIs and AOAs and probably formed by the same process.

We note that fayalite grains in the Kaba and Mokoia matrices have similar chemical and O-isotopic compositions (Fig. 3; Hua *et al.*, 2002) and initial $^{53}Mn/^{55}Mn$ ratio [$(2.28 \pm 0.37) \times 10^{-6}$; Hua *et al.*, 2003, 2004] to those replacing opaque nodules in the Mokoia chondrules (Hutcheon *et al.*, 1998; Choi *et al.*, 2000). Based on these observations, we infer that both textural occurrences of fayalite formed contemporaneously, during the same process—fluid-assisted metamorphism.

Ferrous olivines overgrowing chondrules and chondrule fragments in the CV_{oxA-B} chondrite MET00430 (Fig. 8) show inverse compositional zoning (Fa_{75-50}). An individual ferrous olivine grain overgrowing chondrule pyroxene shown in Fig. 8d has a complex Fe-Mg zoning (Fa_{70-82}). This zoning could have resulted from dissolution-precipitation of ferrous olivine from a fluid which composition was changing with time. Multiple cycles of dissolution-precipitation of ferrous olivine from an aqueous solution may explain the increase of matrix olivine grain sizes and the decrease of their compositional ranges from the CV_{oxB} to CV_{oxA-B} to CV_{oxA} chondrites (Fig. 1; Krot *et al.*, 1998a).

Due to their more extensive alteration, there is no clear textural evidence for direct precipitation of ferrous olivine from a fluid phase in the CV_{oxA} chondrites (in contrast to the secondary Ca,Fe-rich minerals; *e.g.*, Krot *et al.*, 1998b, 2001; MacPherson and Krot, 2002). However, this mechanism is implied by Imai and Yurimoto (2003) to explain oxygen isotope heterogeneity in an Allende AOA (Fig. 9). Oxygen isotopic compositions of the primary forsteritic olivine (Fa_{95}), spinel and fassaite in this AOA are ^{16}O-rich ($\Delta^{17}O \sim -20\text{‰}$ to -25‰), whereas those of the secondary ferrous olivine (Fa_{40}), nepheline and phyllosilicates are ^{16}O-poor ($\Delta^{17}O \sim -5\text{‰}$). Imai and Yurimoto (2003) concluded that the alteration and ^{16}O-poor compositions of the secondary nepheline, phyllosilicates, and ferrous olivine in AOA resulted from aqueous alteration; ferrous olivine directly precipitated from a fluid.

3.4. Dehydration of phyllosilicates

Formation of ferrous olivine by dehydration of phyllosilicates has previously been inferred from the fibrous textures of some of the ferrous olivines in an Allende dark inclusion (Kojima and Tomeoka, 1996), and from the presence of PGC and pentlandite
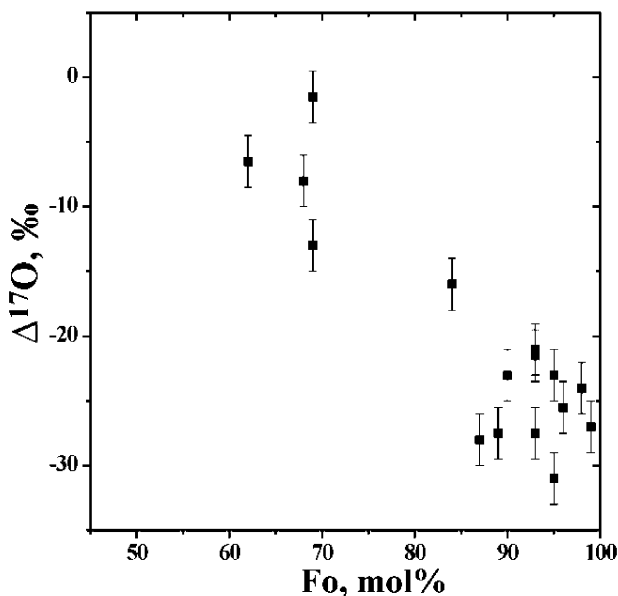
Fig. 9.   *Fayalite (mol%) vs. $\Delta^{17}O$ in olivine in the Allende AOAs (from Imai and Yurimoto, 2003).*

inclusions in the Allende matrix olivines (Brearley, 1999).   Krot *et al*. (1995, 1997) applied this model to explain the origin of secondary ferrous olivine in the oxidized CV chondrites and Allende dark inclusions.   However, the rarity of fibrous olivines, the high abundance of ferrous olivine in the aqueously-altered and virtually un-metamorphosed CV_{oxB} chondrites, and the lack of oxygen-isotopic evidence for extensive hydration-dehydration of the CV chondrites (Clayton and Mayeda, 1999) suggest that a direct substitution of olivine for phyllosilicates has played a minor (if any) role in the origin of ferrous olivine.   Growth of ferrous olivine in the presence of fluid released during dehydration of phyllosilicates seems more likely.

3.5.   *Implications for the origin of matrix ferrous olivine*

The primitive (unaltered and unmetamorphosed) chondritic meteorites (*e.g.*, un-grouped carbonaceous chondrite Acfer 094) and anhydrous interplanetary dust particles lack crystalline ferrous olivine in their matrices, which are dominated by the amorphous Fe-rich silicates and crystalline magnesium-rich olivines and pyroxenes instead (*e.g.*, Greshake, 1997; Bradley, 2003).   In contrast, most type 3 ordinary and carbonaceous chondrites, which experienced alteration of various degrees, lack amorphous material and contain abundant ferrous olivine in their matrices (Scott and Krot, 2003).   This might imply that matrix ferrous olivine has predominantly an asteroidal origin.   More work is required to test this hypothesis.
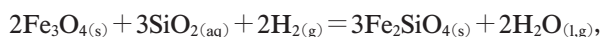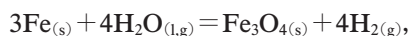
4.   Conclusions and implications

It has previously been suggested that fibrous ferrous olivine in dark inclusions in CV
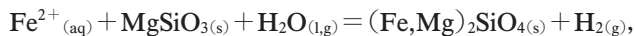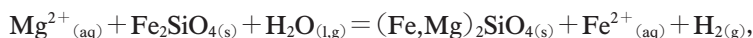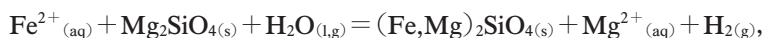
chondrites formed by dehydration of phyllosilicates during thermal metamorphism (Kojima and Tomeoka, 1996; Krot *et al.*, 1995). This mechanism has been subsequently applied to explain the origin of ferrous olivine in the CV chondrules and matrices (Krot *et al.*, 1997). However, this mechanism is inconsistent with the lack of significant fractionation of bulk oxygen isotope compositions of the CV chondrites and the Allende dark inclusions and the common occurrences of ferrous olivine in the aqueously-altered and virtually unmetamorphosed oxidized CV chondrites of the Bali-like subgroup.

Based on the petrographic observations and isotopic compositions of the ferrous olivine and the coexisting secondary minerals (Ca,Fe-pyroxenes, andradite, magnetite), we infer that secondary ferrous olivine in CV chondrites formed during fluid-assisted thermal metamorphism by several mechanisms:

(*i*) replacement of Fe,Ni-metal $\pm$ sulfide nodules:

$$3Fe_{(s)} + 4H_2O_{(l,g)} = Fe_3O_{4(s)} + 4H_{2(g)},$$

$$2Fe_3O_{4(s)} + 3SiO_{2(aq)} + 2H_{2(g)} = 3Fe_2SiO_{4(s)} + 2H_2O_{(l,g)},$$

(*ii*) replacement of magnesian olivine and pyroxene:

$$Fe^{2+}_{(aq)} + Mg_2SiO_{4(s)} + H_2O_{(l,g)} = (Fe,Mg)_2SiO_{4(s)} + Mg^{2+}_{(aq)} + H_{2(g)},$$

$$Mg^{2+}_{(aq)} + Fe_2SiO_{4(s)} + H_2O_{(l,g)} = (Fe,Mg)_2SiO_{4(s)} + Fe^{2+}_{(aq)} + H_{2(g)},$$

$$Fe^{2+}_{(aq)} + MgSiO_{3(s)} + H_2O_{(l,g)} = (Fe,Mg)_2SiO_{4(s)} + H_{2(g)},$$

and (*iii*) direct precipitation from an aqueous solution:

$$Fe^{2+}_{(aq)} + Mg^{2+}_{(aq)} + SiO_{2(aq)} = (Fe,Mg)_2SiO_{4(s)}.$$

Although formation of ferrous olivine by dehydration of phyllosilicates cannot be entirely excluded, it probably played only a minor (if any) role.

References

Aléon, J., Krot, A.N. and McKeegan, K.D. (2002): Calcium-aluminum-rich inclusions and amoeboid olivine aggregates from the CR carbonaceous chondrites. Meteorit. Planet. Sci., **37**, 1729–1755.

Amelin, Y., Krot, A.N., Hutcheon, I.D. and Ulyanov, A.A. (2002): Lead isotopic ages of chondrules and calcium-aluminum-rich inclusions. Science, **297**, 1678–1683.

Bland, P. A., Hoffman, E., Krot, A.N. and Berry, F. J. (2000): CV3 chondrites; how oxidized or reduced? (abstract). Meteorit. Planet. Sci., **35** (Suppl.), A28.

Boss, A.P. (2003): The solar nebula. Meteorites, Comets, and Planets, ed. by A.M. Davis. Oxford, Elsevier-Pergamon, 63–83 (Treatise on Geochemistry, ed. by H.D. Holland and K.K. Turekian, Vol. 1).

Bradley, J.P. (2003): Interplanetary dust particles. Meteorites, Comets, and Planets, ed. by A.M. Davis. Oxford, Elsevier-Pergamon, 689–713 (Treatise on Geochemistry, ed. by H.D. Holland and K.K. Turekian, Vol. 1).

Brearley, A.J. (1997): Disordered biopyriboles, amphibole, and talc in the Allende Meteorite; products of nebular or parent body aqueous alteration? Science, **276**, 1103–1105.

Brearley, A.J. (1998): Dark inclusions in the Leoville CV3 carbonaceous chondrite. Lunar and Planetary Science XXIX. Houston, Lunar Planet. Inst., Abstract #1245 (CD-ROM).

Brearley, A.J. (1999): Origin of graphitic carbon and pentlandite in matrix olivines in the Allende meteorite. Science, **285**, 1380–1382.

Brearley, A.J. (2003): Nebular *vs*. parent-body processing. Meteorites, Comets, and Planets, ed. by A.M. Davis. Oxford, Elsevier-Pergamon, 247–269 (Treatise on Geochemistry, ed. by H.D. Holland and K.K. Turekian, Vol. 1).

Brearley, A.J. and Jones, R.H. (1998): Chondritic meteorites. Planetary Materials, ed. by J.J. Papike. Washington, D.C., Mineral. Soc. Am., 3-1-3-398 (Reviews in Mineralogy, Vol. 36).

Brearley, A.J. and Hutcheon, I.D. (2000): Carbonates in the CM1 chondrite ALH84034: Mineral chemistry, zoning and Mn-Cr systematics (abstract). Lunar and Planetary Science XXXI. Houston, Lunar Planet. Inst., Abstract #1407 (CD-ROM).

Brearley, A.J. and Hutcheon, I.D. (2002): Carbonates in the Y791918 CM2 chondrite: Zoning and Mn-Cr systematics (abstract). Meteorit. Planet. Sci., **37** (Suppl.), A23.

Brearley, A.J. and Shearer, C.K. (2000): Origin of calcium-iron-rich pyroxenes in Allende matrix: Clues from rare-earth-element abundances (abstract). Meteorit. Planet. Sci., **35** (Suppl.), A33.

Brenker, F.E. and Krot, A.N. (2004): Late-stage, high-temperature processesing in the Allende meteorite: Record from Ca,Fe-rich silicate rims around dark inclusions. Am. Mineral., **89**, 1280–1289.

Brenker, F.E., Klerner, S. and Palme, H. (2000): Evidence for solar nebular signatures in the matrix of the Allende meteorite. Earth Planet. Sci. Lett., **178**, 185–194.

Buchanan, P.C., Zolensky, M.E. and Reid, A.M. (1997): Petrology of Allende dark inclusions. Geochim. Cosmochim. Acta, **61**, 1733–1743.

Choi, B.-G., Krot, A.N. and Wasson, J.T. (2000): Oxygen-isotopes in magnetite and fayalite in CV chondrites Kaba and Mokoia. Meteorit. Planet. Sci., **35**, 1239–1249.

Clayton, R.N. and Mayeda, T.K. (1999): Oxygen isotope studies of carbonaceous chondrites. Geochim. Cosmochim. Acta, **63**, 2089–2104.

Cosarinsky, M., Leshin, L.A., MacPherson, G.J., Krot, A.N. and Guan, Y. (2003): Oxygen isotope composition of Ca-Fe-rich silicates in and around al Allende Ca-Al-rich inclusion. Lunar and Planetary Science XXXIV. Houston, Lunar Planet. Inst., Abstract #1043 (CD-ROM).

Dohmen, R., Chakraborty, S., Palme, H. and Rammensee, W. (1998): Solid-solid reactions mediated by a gas phase; an experimental study of reaction progress and the role of surfaces in the system olivine + iron metal. Am. Mineral., **83**, 970–984.

Fruland, R.M., King, A.E. and McKay, D.S. (1978): Allende dark inclusions. Proc. Lunar Planet. Sci. Conf., **9th**, 1305–1329.

Greshake, A. (1997): The primitive matrix components of the unique carbonaceous chondrite Acfer 094; a TEM study. Geochim. Cosmochim. Acta, **61**, 437–452.

Hashimoto, A. and Grossman, L. (1987): Alteration of Al-rich inclusions inside amoeboid olivine aggregates in the Allende meteorite. Geochim. Cosmochim. Acta, **51**, 1685–1704.

Hua, X. and Buseck, P.R. (1995): Fayalite in the Kaba and Mokoia carbonaceous chondrites. Geochim. Cosmochim. Acta, **59**, 563–579.

Hua, X., Huss, G.R. and Sharp, T.G. (2002): [53]Mn-[53]Cr dating of fayalite formation in the Kaba CV3 carbonaceous chondrite. Lunar and Planetary Science XXXIII. Houston, Lunar Planet. Inst., Abstract #1660 (CD-ROM).

Hua, X., Huss, G.R., Tachibana, S. and Sharp, T.G. (2003): Oxygen isotopic compositions of fayalite in the Kaba CV3 carbonaceous chondrite. Lunar and Planetary Science XXXIV. Houston, Lunar Planet. Inst., Abstract #1702 (CD-ROM).

Hua, X., Huss, G.R., Tachibana, S. and Sharp, T.G. (2004): Oxygen, Si, and Mn-Cr isotopes of fayalite in the oxidized Kaba CV3 chondrite: Constraints for its formation history. submitted to Geochim. Cosmochim. Acta.

Hutcheon, I.D., Krot, A.N., Keil, K., Phinney, D.L. and Scott, E.R.D. (1998): ^{53}Mn-^{53}Cr dating of fayalite formation in the CV3 chondrite Mokoia: Evidence for asteroidal alteration. Science, **282**, 1865–1867.

Imai, H. and Yurimoto, H. (2003): Oxygen isotopic distribution in an amoeboid olivine aggregate from the Allende CV chondrite: Primary and secondary processes. Geochim. Cosmochim. Acta, **67**, 765–772.

Johnson, C.A., Prinz, M., Weisberg, M.K., Clayton, R.N. and Mayeda, T.K. (1990): Dark inclusions in Allende, Leoville, and Vigarano: Evidence for nebular oxidation of CV3 constituents. Geochim. Cosmochim. Acta, **54**, 819–831.

Jones, R.H. and Scott, E.R.D. (1989): Petrology and thermal history of type IA chondrules in the Semarkona (LL3.0) chondrite. Proc. Lunar Planet. Sci. Conf., **19th**, 523–536.

Kimura, M. and Ikeda, Y. (1995): Anhydrous alteration of Allende chondrules in the solar nebula; II, Alkali-Ca exchange reactions and formation of nepheline, sodalite and Ca-rich phases in chondrules. Proc. NIPR Symp. Antarctic Meteorites, **8**, 123–138.

Kimura, M. and Ikeda, Y. (1998): Hydrous and anhydrous alterations of chondrules in Kaba and Mokoia CV chondrites. Meteorit. Planet. Sci., **33**, 1139–1146.

Kojima, T. and Tomeoka, K. (1996): Indicators of aqueous alteration and thermal metamorphism on the CV3 parent body: Microtextures of a dark inclusion from Allende. Geochim. Cosmochim. Acta, **60**, 2651–2666.

Kracher, A., Keil, K., Kallemeyn, G.W., Wasson J.T., Clayton R.N. and Huss G.R. (1985): The Leoville (CV3) accretionary breccia. Proc. Lunar Planet. Sci. Conf., 16th, Pt. 1, D123–D135 (J. Geophys. Res., **90** Suppl.).

Krot, A.N. and Todd, C.S. (1998): Metal-carbide-magnetite-fayalite association in a Bali-like clast in the reduced CV3 chondrite breccia Vigarano (abstract). Meteorit. Planet. Sci., **34** (Suppl.), A88–A89.

Krot, A.N., Scott, E.R.D. and Zolensky, M.E. (1995): Mineralogic and chemical variations among CV3 chondrites and their components: Nebular and asteroidal processing. Meteoritics, **30**, 748–775.

Krot, A.N., Scott, E.R.D. and Zolensky, M.E. (1997): Origin of fayalitic olivine rims and plate-like matrix olivine in the CV3 chondrite Allende and its dark inclusions. Meteoritics, **32**, 31–49.

Krot, A.N., Petaev, M.I., Scott, E.R.D., Choi B.-G., Zolensky M.E. and Keil K. (1998a): Progressive alteration in CV3 chondrites: More evidence for asteroidal alteration. Meteorit. Planet. Sci., **33**, 1065–1085.

Krot, A.N., Zolensky, M.E., Keil, K., Scott, E.R.D. and Nakamura, K. (1998b): Secondary Ca-Fe-rich minerals in the Bali-like and Allende-like oxidized CV3 chondrites and Allende dark inclusions. Meteorit. Planet. Sci., **33**, 623–645.

Krot, A.N., Brearley, A.J., Ulyanov, A.A., Biryukov, V.V., Swindle, T.D., Keil, K., Mittlefehldt, D.W., Scott, E.R.D., Clayton, R.N. and Mayeda, T.K. (1999): Mineralogy, petrography and bulk chemical, I-Xe, and oxygen isotopic compositions of dark inclusions in the reduced CV3 chondrite Efremovka. Meteorit. Planet. Sci., **34**, 67–89.

Krot, A.N., Meibom, A. and Keil, K. (2000a): A clast of Bali-like oxidized CV3 material in the reduced CV 3 chondrite breccia Vigarano. Meteorit. Planet. Sci., **35**, 817–827.

Krot, A.N., Hiyagon, H., Petaev, M.I. and Meibom, A. (2000b): Oxygen isotopic compositions of secondary Ca-Fe-rich silicates from the Allende dark inclusions: Evidence against high-temperature formation. Lunar and Planetary Science XXXI. Houston, Lunar Planet. Inst., Abstract #1463 (CD-ROM).

Krot, A.N., Brearley, A.J., Petaev, M.I., Kallemeyn, G.W., Sears, D.W.G., Benoit, P.H., Hutcheon, I.D., Zolensky, M.E. and Keil, K. (2000c): Evidence for in situ growth of fayalite and hedenbergite in MacAlpine Hills 88107, ungrouped carbonaceous chondrite related to CM-CO clan. Meteorit. Planet. Sci., **35**, 1365–1387.

Krot, A.N., Petaev, M I., Meibom, A. and Keil, K. (2001): *In situ* growth of Ca-rich rims around Allende dark inclusions. Geochem. Int., **36**, 351–368.

Krot, A.N., Hohenberg, C.M., Meshik A.P., Pravdivtseva, O.V., Hiyagon, H., Petaev M.I., Weisberg, M.K., Meibom, A. and Keil, K. (2002): Two-stage alteration of the Allende dark inclusions (abstract). Meteorit. Planet. Sci., **37** (Suppl.), A82.

Krot, A.N., Petaev, M. I. and Bland, P.A. (2003a): Growth of ferrous olivine in the oxidized CV chondrites during fluid-assisted thermal metamorphism (abstract). Meteorit. Planet. Sci., **38** (Suppl.), A73.

Krot, A.N., Petaev, M.I. and Bland, P.A. (2003b): Multiple formation mechanisms of ferrous olivine in CV 3 carbonaceous chondrites during fluid-assisted metamorphism (abstract). International Symposium Evolution of Solar System Materials: A New Perspective from Antarctic Meteorites. Tokyo, Natl Inst. Polar Res., 61–62.

Krot A.N., Hutcheon, I.D., Brearley, I.D., Petaev M.I., Pravdivtseva O.V. and Hohenberg, C.M. (2003c): Timescales of the secondary alteration of chondritic meteorites. submitted to Meteorites and the Early Solar System II, ed. by D. Lauretta *et al*. University of Arizona Press.

Krot, A.N., MacPherson, G.J., Ulyanov, A.A. and Petaev, M.I. (2004): Fine-grained, spinel-rich inclusions from the reduced CV chondrites Efremovka and Leoville: I. Mineralogy, petrology, and bulk chemistry. Meteorit. Planet. Sci., **39**, 1517–1553.

Kurat, G., Palme, H., Brandstätter, F. and Huth, J. (1989): Allende xenolith AF: Undisturbed record of condensation and aggregation of matter in the solar nebula. Z. Naturforsch., **44a**, 988–1004.

Lugmair, G.W. and Shukolyukov, A. (1998): Early solar system timescales according to ^{53}Mn-^{53}Mn systematics. Geochim. Cosmochim. Acta, **62**, 2863–2886.

MacPherson, G.J. and Krot, A.N. (2002): Distribution of Ca-Fe-silicates in CV3 chondrites: Possible controls by parent body compaction (abstract). Meteorit. Planet. Sci., **37** (Suppl.), A91.

McSween, H.Y., Jr. (1977): Petrographic variations among carbonaceous chondrites of the Vigarano type. Geochim. Cosmochim. Acta, **41**, 1777–1790.

Palme, H. and Wark, D.A. (1988): CV-chondrites; high temperature gas-solid equilibrium *vs*. parent body metamorphism (abstract). Lunar and Planetary Science XIX. Houston, Lunar Planet. Inst., 897–898.

Podosek, F.A. and Cassen, P. (1994): Theoretical, observational, and isotopic estimates of the lifetime of the solar nebula. Meteoritics, **29**, 6–25.

Pravdivtseva, O.V. and Hohenberg, C.M. (2001): The I-Xe system of magnetic fractions from CV3 meteorites. Lunar and Planetary Science XXXII. Houston, Lunar Planet. Inst., Abstract #2176 (CD-ROM).

Pravdivtseva, O.V., Hohenberg, C.M., Meshik A.P. and Krot A.N. (2001): I-Xe ages of different mineral fractions from Bali and Kaba (CV3) (abstract). Meteorit. Planet. Sci., **36** (Suppl.), A168.

Pravdivtseva, O.V., Krot, A.N., Hohenberg, C.M., Meshik, A.M., Weisberg, M.K. and Keil, K. (2003a): The I-Xe record of alteration in the Allende CV chondrite. Geochim. Cosmochim. Acta, **67**, 5011–5026.

Pravdivtseva, O.V., Hohenberg, C.M., Meshik, A.M., Krot, A.N. and Brearley, A.J. (2003b): I-Xe age of the dark inclusions from the reduced CV3 chondrites Leoville, Efremovka, and Vigarano (abstract). Meteorit. Planet. Sci., **38** (Suppl.), A140.

Scott, E.R.D. and Krot, A.N. (2003): Chondrites and their components. Meteorites, Comets, and Planets, ed. by A.M. Davis. Oxford, Elsevier-Pergamon, 143–201 (Treatise on Geochemistry, ed. by H.D. Holland and K.K. Turekian, Vol. 1).

Scott, E.R.D., Keil, K. and Stöffler, D. (1992): Shock metamorphism of carbonaceous chondrites. Geochim. Cosmochim. Acta, **56**, 4281–4293.

Weisberg, M.K. and Prinz, M. (1998): Fayalitic olivine in CV3 chondrite matrix and dark inclusions: A nebular origin. Meteorit. Planet. Sci., **33**, 1087–1111.

Weisberg, M.K., Prinz, M., Clayton, R.N. and Mayeda, T.K. (1997): CV3 chondrites; three subgroups, not two (abstract). Meteorit. Planet. Sci., **32** (Suppl.), A138–A139.